

Does increasing the number of channels during neuromuscular electrical stimulation reduce fatigability and produce larger contractions with less discomfort?

Trevor Scott Barss (✉ tbarss@ualberta.ca)

University of Alberta <https://orcid.org/0000-0003-3466-2750>

Bailey WM Sallis

University of Alberta

Dylan J Miller

University of Alberta

David F Collins

University of Alberta

Original Article

Keywords: functional electrical stimulation, neuromuscular electrical stimulation, sequential, motor unit, fatigability, evoked contractions, rehabilitation, muscle

Posted Date: January 29th, 2021

DOI: <https://doi.org/10.21203/rs.3.rs-164031/v1>

License: © ⓘ This work is licensed under a Creative Commons Attribution 4.0 International License.

[Read Full License](#)

1
2
3
4
5
6
7
8
9
10
11
12
13
14
15
16
17
18
19
20
21
22
23
24
25
26
27
28
29
30
31
32
33
34
35
36
37

Does increasing the number of channels during neuromuscular electrical stimulation reduce fatigability and produce larger contractions with less discomfort?

Trevor S. Barss, Bailey W.M. Sallis, Dylan J. Miller, David F. Collins

Human Neurophysiology Laboratory, Faculty of Kinesiology, Sport, and Recreation,
Neuroscience and Mental Health Institute, University of Alberta, Edmonton, Alberta, Canada.

Running Head: Multi-channel NMES: fatigability, torque, discomfort

Correspondence:
David F Collins
Human Neurophysiology Laboratory,
Faculty of Kinesiology, Sport, and Recreation
4-219 Van Vliet Complex
University of Alberta, Edmonton, Alberta
Canada, T6G 2H9
Phone: 780.492.6506
Email: dcollins@ualberta.ca

38 **ABSTRACT:**

39 **Purpose:** Neuromuscular electrical stimulation (NMES) recruits motor units (MUs) at
40 unphysiologically high rates, leading to contraction fatigability. Rotating NMES pulses between
41 multiple electrodes recruits different MUs from each site, reducing MU firing rates and
42 fatigability. This study was designed to determine whether rotating pulses between an increasing
43 number of stimulation channels (cathodes) reduces contraction fatigability and increases the
44 ability to generate torque during NMES. A secondary outcome was perceived discomfort.

45 **Methods:** Fifteen neurologically-intact volunteers completed 4 sessions. NMES was delivered
46 over the quadriceps through 1 (NMES₁), 2 (NMES₂), 4 (NMES₄) or 8 (NMES₈) channels.

47 Fatigability was assessed over 100 contractions (1s on/1s off) at an initial contraction amplitude
48 that was 20% of a maximal voluntary contraction (MVC). Torque-frequency relationships were

49 characterized over 6 frequencies from 20-120Hz. **Results:** NMES₄ and NMES₈ resulted in less
50 decline in torque (42% and 41 %) and generated more torque over the 100 contractions than

51 NMES₁ and NMES₂ (53% and 50% decline in torque). Increasing frequency from 20-120Hz
52 increased torque by 7, 13, 21 and 24% MVC, for NMES₁, NMES₂, NMES₄ and NMES₈,

53 respectively. Perceived discomfort was highest during NMES₈. **Conclusion:** NMES₄ and

54 NMES₈ reduced contraction fatigability and generated larger contractions across a range of

55 frequencies than NMES₁ and NMES₂. NMES₈ produced the most discomfort, likely due to small

56 electrodes and high current density. During NMES, more is not better and rotating pulses

57 between 4 channels may be optimal to reduce contraction fatigability and produce larger

58 contractions with minimal discomfort compared to conventional NMES configurations.

59

60

61 **KEYWORDS:** functional electrical stimulation; neuromuscular electrical stimulation;
62 sequential; motor unit; fatigability; evoked contractions; rehabilitation; muscle
63
64 **DECLARATIONS:**
65 **FUNDING:** This work was supported with a Craig H. Neilsen Foundation Senior Research
66 Grant (DFC) and a Campus Alberta Neuroscience Postdoctoral Fellowship (TSB).
67 **CONFLICTS OF INTEREST:** The authors have no conflict of interest to report.
68 **AVAILABILITY OF DATA AND MATERIAL:** Not Applicable.
69 **CODE AVAILABILITY:** Not applicable.
70 **AUTHOR CONTRIBUTIONS:** AUTHOR CONTRIBUTIONS: Experiments were conducted
71 in the Human Neurophysiology Laboratory at the University of Alberta. Trevor S. Barss, Bailey
72 W.M. Sallis and Dave F. Collins contributed to the conception and experimental design. Trevor
73 S. Barss, Bailey W.M. Sallis and Dylan J. Miller collected and analyzed the data. Trevor S.
74 Barss, Bailey W.M. Sallis and Dave F. Collins contributed to the interpretation and drafting of
75 the manuscript. Trevor S. Barss, Bailey W.M. Sallis, Dylan J. Miller and Dave F. Collins
76 provided revisions for and approved the final draft of the manuscript.
77 **ETHICS APPROVAL AND CONSENT TO PARTICIPATE:** Participants provided informed
78 written consent and procedures were approved by the University of Alberta Research Ethics
79 Board (Pro00078696) and in accordance with the 1964 Declaration of Helsinki.
80 **ACKNOWLEDGMENTS:** The authors would like to thank Mr. Alejandro Ley and Zoltan
81 Kenwell for their technical support.

82

83

84 **ABBREVIATIONS**

85 SDSS - Spatially-distributed sequential stimulation

86 EMG – Electromyography

87 MU – Motor unit

88 MVC – Maximum voluntary contraction

89 NMES - Neuromuscular electrical stimulation

90 VAS – Visual analog scale

91

92

93

94

95

96

97

98

99

100

101

102

103

104

105

106

107 **INTRODUCTION**

108 Neuromuscular electrical stimulation (NMES) evokes contractions when pulses of
109 current are applied through electrodes on the skin and it is used in diverse applications to
110 enhance or maintain neuromuscular function (Sheffler and Chae 2007; Bickel et al. 2011). Long-
111 term benefits of NMES-based programs after neurotrauma include reduced muscle atrophy and
112 spasticity with increased muscle strength, bone mineral density and cardiovascular fitness
113 (Bélanger et al. 2000; Davis et al. 2008; Griffin et al. 2009). For many applications the large
114 knee-extensor muscles (quadriceps) are stimulated using a single channel comprising of two
115 electrodes over the muscle belly, an “active” cathode and a “return” anode (Maffiuletti 2010;
116 Bergquist et al. 2011). Due to the non-physiological way motor units (MUs) are recruited during
117 this type of NMES, however, with superficial MUs discharging synchronously at high rates and
118 in a non-physiological order, it can be difficult to produce contractions of sufficient amplitude
119 and contractions fatigue rapidly (Barss et al. 2018). Contraction fatigability and the inability to
120 produce sufficient torque limits the benefits of NMES programs by shortening the duration and
121 intensity of NMES sessions (Kluger et al. 2013).

122 One way to reduce contraction fatigability during NMES is by rotating stimulation pulses
123 between multiple electrodes. Rotating pulses between electrodes distributed over a muscle belly
124 recruits MUs in different parts of the muscle sequentially, not synchronously, decreasing firing
125 rates (Nguyen et al. 2011; Sayenko et al. 2014). This type of NMES has been given various
126 names, the most descriptive of which may be spatially-distributed sequential stimulation (SDSS).
127 SDSS reduces fatigability of contractions of tibialis anterior (Wiest et al. 2019) and the triceps
128 surae (Nguyen et al. 2011) in neurologically intact participants and of the quadriceps in both
129 neurologically intact participants (Bergquist et al. 2017; Laubacher et al. 2017) and those who

130 have experienced a spinal cord injury (Popović and Malešević 2009; Malešević et al. 2010;
131 Nguyen et al. 2011; Laubacher et al. 2019). For SDSS approaches to work effectively, different
132 pools of MUs must be recruited by each stimulation channel, with little if any overlap of MUs
133 recruited by adjacent channels. Thus far the evidence suggests that to reduce contraction
134 fatigability more NMES channels are better, however, little work has been done to determine
135 how many channels are optimal.

136 The inability to produce sufficient torque during conventional NMES is another major
137 barrier to its wide-spread use that SDSS may be able to address. During SDSS, when different
138 MUs are recruited from each stimulation site, as the number of stimulation channels increases
139 more MUs are recruited at lower frequencies to produce a given contraction amplitude. For
140 example, to produce 20% of the torque produced during an MVC, conventional one-channel
141 NMES delivered at 40 Hz might recruit 1000 MUs synchronously at 40 Hz, whereas to produce
142 the same amount of torque four-channel SDSS delivered at 40 Hz might recruit 4000 MUs in 4
143 separate groups, each at 10 Hz. Thus, one limitation of conventional one-channel NMES is that it
144 must be delivered at relatively high frequencies to produce sufficiently large contractions. The
145 resulting high discharge rates place MUs at the high end of the curve that describes the
146 relationship between torque and discharge frequency, leaving little if any room to increase torque
147 with further increases in NMES frequency. As the number of stimulation channels increases, and
148 MU firing rates decrease (see above), however, MUs shift progressively leftward on the torque-
149 frequency curve, potentially leaving a much larger range over which NMES frequency can be
150 used to modulate torque. Thus, as the number of NMES channels increases, there may be an
151 opportunity to increase NMES frequency and generate larger contractions while keeping MU
152 firing rates in their physiological range to minimize contraction fatigability. The relationship

153 between torque and NMES frequency when stimulating through multiple channels, however, has
154 not been established.

155 Therefore, the primary purpose of this study was to determine the effect of rotating
156 NMES pulses through an increasing number of NMES channels on contraction fatigability and
157 the ability to generate torque across a range of frequencies. Given that discomfort plays a role in
158 the clinical application of NMES (Fukuda et al. 2013) perceived discomfort was a secondary
159 outcome measure. NMES was delivered over the quadriceps muscles through 1 (NMES₁), 2
160 (NMES₂), 4 (NMES₄) and 8 (NMES₈) channels and outcome measures were assessed over a
161 series of intermittent isometric contractions of a fatigue protocol. We hypothesized that as the
162 number of channels progressively increased, contraction fatigability would progressively
163 decrease. Thus, we predicted that torque would decline the most during NMES₁ and would
164 decline progressively less as the number of cathodes increased. We also hypothesized that
165 increasing the number of channels would increase evoked torque across a range of stimulation
166 frequencies. Thus, we predicted that when NMES frequency increased from 20-120 Hz torque
167 would increase the least during NMES₁, with progressively greater increases in torque across the
168 range of frequencies as the number of channels increased. The results of these experiments will
169 help identify the optimal number of stimulation channels for NMES of the quadriceps muscles to
170 generate large, fatigue-resistant, contractions with the least discomfort.

171

172 **METHODS**

173 *Participants*

174 Fifteen neurologically intact participants (5 women, 10 men; aged 28.5 ± 12.0 years,
175 range 18-55 years) completed 4 sessions. A different type of NMES was tested in each session

176 and the order of sessions was randomised for each participant. Sessions lasted approximately 45
177 minutes and were separated by a minimum of 48 hours. Participants provided informed written
178 consent and procedures were approved by the University of Alberta Research Ethics Board.

179

180 *Torque*

181 Isometric knee extension torque produced by the right leg was measured while
182 participants sat in the chair of a Biodex dynamometer (System 3, Biodex Medical Systems,
183 Shirley, New York, USA). The leg was secured to maintain a knee angle of $\sim 100^\circ$ and the fibular
184 head was aligned with the axis of the dynamometer.

185

186 *Neuromuscular Electrical Stimulation (NMES)*

187 A constant current DS7AH stimulator (Digitimer, Welwyn Garden City, UK) was used to
188 deliver one ms square wave pulses of current through self-adhesive electrodes (Large 2"x 4" and
189 Small 2"x 2"; UltraStim; Axelgaard Manufacturin Co., Fallbrook, CA, USA) over the
190 quadriceps. A custom-built system was used to distribute stimulus pulses to the appropriate
191 electrode pairs. NMES₁, NMES₂, NMES₄, and NMES₈ were delivered through 1, 2, 4 or 8 active
192 electrodes (cathodes), respectively, as shown in Figure 1A. These configurations are described
193 below and were chosen based on the results of pilot studies designed to reduce fatigability by
194 recruiting different MUs with each cathode.

195 For all configurations one large electrode was placed ~ 2 -4 cm from the proximal edge of
196 the patella centered over the midline of the quadriceps and another ~ 3 -5 cm from the inguinal
197 crease centered over the midline of the quadriceps. NMES₁: One large cathode was placed near
198 the hip and one large anode was placed near the knee as described above. NMES₂: Same

199 configuration as for NMES₁ although the anode and the cathode alternated between electrodes 1
200 and 2 with every other pulse. NMES₄: Four large cathodes were placed in a rectangular pattern in
201 the middle of the thigh (electrodes 1-4), between anodes (electrodes A and B). The proximal
202 cathodes (1 and 3) were paired with the distal anode (A) and the distal cathodes (2 and 4) were
203 paired with the proximal anode (B). Stimulus pulses were rotated sequentially through the
204 numbered electrodes shown in Figure 1A. NMES₈: Due to space limitations on the thigh large
205 electrodes could not be used, thus small cathodes were placed in a 2x4 array (1-8) between the
206 anodes (A and B). Pulses were rotated sequentially through electrode pairs as shown in Figure
207 1A with proximal cathodes (1, 3, 5, and 7) being paired with the distal anode (A) and the distal
208 cathodes (2, 4, 6, and 8) being paired with the proximal cathode (B). Skin was prepared using
209 alcohol swabs before placement of the electrodes. Current was measured with a current probe
210 from channel 1 during all trials (mA- 2000, F.W. Bell).

211

212 *General Protocol*

213 As shown in Figure 1B, each session began with maximal voluntary contractions
214 (MVCs) followed by collection of data to generate the torque-frequency curves. Participants then
215 completed the fatigue protocol followed by another MVC (details described below).

216

217 *Maximal Voluntary Contractions (MVCs)*

218 Participants performed isometric knee extension MVCs for 2-3s with verbal
219 encouragement and visual feedback of torque provided throughout. Each participant performed 2
220 MVCs separated by a minimum of 1 minute with a 3rd MVC being completed if the first 2
221 varied by more than 10%. The MVC that elicited the most torque was used to normalize all

222 subsequent torque measurements. Another MVC was performed within one minute after the
223 fatigue protocol. Torque recorded during MVCs was quantified as the average torque over a 0.3 s
224 window centered on the peak.

225

226 *Torque-Frequency Relationships*

227 The relationship between torque and frequency was characterized for each NMES
228 configuration. One second trains (n=2) of each type of NMES were delivered at 20, 40, 60, 80,
229 100, and 120 Hz at an intensity that generated 20% MVC at 40 Hz. Trains were separated by at
230 least 5 seconds and the order of the 12 stimulation trains for each configuration was randomised
231 for each participant. Peak torque was calculated over a 10 ms window centered around the peak
232 and was normalized to each participants' MVC. Perceived discomfort was assessed during the
233 first contraction of each frequency. Discomfort scores were provided verbally by the participant
234 using a Visual Analogue Scale (VAS) with endpoints ranging from 0 (no pain) to 100 (worst
235 pain imaginable).

236

237 *Fatigue Protocol*

238 For each fatigue protocol NMES was delivered at 40 Hz to evoke 100 contractions using
239 a 1 second on, 1 second off duty cycle. Stimulus intensity was adjusted to generate contractions
240 that produced 20% MVC torque at the beginning of the fatigue protocol. Two measures of
241 contraction amplitude were used; Peak torque was calculated as described above (see *Torque-*
242 *frequency Relationships*) and the torque-time integral (TTI) was calculated as the area under the
243 torque versus time curve for each contraction. All data were averaged into bins representing 10
244 successive contractions, resulting in a total of 10 bins. Fatigability was assessed using five

245 outcome measures: 1) percent decline in mean torque from bin 1 to bin 10, 2) percent decline in
246 TTI from bin 1 to bin 10, 3) mean torque across all 100 contractions, 4) mean TTI across all 100
247 contractions and, 5) percent decline in MVC torque from before to after the fatigue protocols.
248 Discomfort scores were recorded (as described above) during the 5th, 50th and 100th contractions.
249 Current (in mA) was also measured and current density was calculated based on electrode area.

250

251 *Data Acquisition*

252 Data were acquired using custom written LabVIEW software (National Instruments,
253 Austin, Texas) sampled at 2000 Hz and stored for later analyses using MATLAB (The
254 Mathworks, Natick, Massachusetts) custom-written software.

255

256 *Statistical analyses*

257 Statistical analyses were conducted on group data. To compare fatigability between
258 NMES configurations, the five outcome measures were tested using separate 1 x 4 (NMES
259 configuration; NMES₁, NMES₂, NMES₄, NMES₈) analyses of variance (ANOVAs). To compare
260 torque across frequencies (20-120 Hz), a 4 (NMES configuration) x 6 (Frequency) rmANOVA
261 was performed. Differences in perceived discomfort during the fatigue protocols were
262 determined using a 3 (Time; beginning, middle, end) x 4 (NMES type) rmANOVA. Differences
263 in perceived discomfort across frequencies (20-120 Hz) were determined using a 4 (NMES
264 configuration) x 6 (Frequency) rmANOVA. To assess differences in current and current density
265 separate 1 x 4 (NMES configuration) ANOVAs were performed. For all ANOVAs, significant
266 interactions were followed by separate analyses for each factor followed by pairwise
267 comparisons using a Bonferroni correction for multiple comparisons. A *p*-value of less than 0.05

268 was considered statistically significant. All data are reported as mean \pm sd. For brevity, only
269 significant results are presented in the Results section and values are included in either text or
270 figures without duplication.

271

272 **RESULTS**

273 *Single participant data*

274 Torque recorded from a single participant during all contractions of each fatigue protocol
275 are shown in Figure 2A and these data, binned over 10 successive contractions, are replotted in
276 Panel B. Over the course of the fatigue protocol for this participant, torque declined by 44%,
277 46%, 38%, and 32% (from bin 1 to bin 10) during NMES₁, NMES₂, NMES₄, and NMES₈,
278 respectively.

279

280 *Group data*

281 *Contraction Fatigability*

282 Figure 3A shows torque recorded during the fatigue protocols, binned and averaged
283 across participants, for each NMES configuration. There were no significant differences in peak
284 torque ($F_{(3, 42)} = 0.414, p = 0.744$) or TTI ($F_{(3, 42)} = 0.709, p = 0.522$) over the first ten contractions
285 of the fatigue protocol (i.e. Bin 1) between any of the NMES configurations. The average initial
286 peak torque and TTI was 18.9% MVC and 11.3% MVC·s, respectively. There was, however, a
287 significant main effect of NMES configuration both for the percent decline in peak torque ($F_{(3, 42)}$
288 $= 8.070, p < 0.001$) and TTI ($F_{(3, 42)} = 9.899, p < 0.001$). Both peak torque (Figure 3B) and TTI
289 (Figure 3C) declined significantly more from bin 1 to bin 10 when using NMES₁ and NMES₂
290 compared to NMES₄ and NMES₈. There was also a significant main effect of NMES

291 configuration for average peak torque ($F_{(3, 42)} = 9.789, p < 0.001$) and TTI ($F_{(3, 42)} = 9.670, p <$
292 0.001). Consistent with percent decline data in panels B and C, there was significantly less mean
293 torque across the entire fatigue protocol when using NMES₁ and NMES₂ compared to NMES₄
294 and NMES₈ (panel D). A similar result was obtained for the mean TTI across the fatigue
295 protocol, with the exception that NMES₈ was not significantly different from NMES₂ (panel E).
296 There were no significant differences in the amount that torque produced during MVCs declined
297 from before to after the fatigue protocols between NMES configurations ($F_{(3,42)} = 0.205,$
298 $p=0.892$; data not shown). The average decline in MVC torque across NMES configurations was
299 $11\pm 6\%$.

300

301 *Torque-Frequency Relationships*

302 Mean torque averaged across participants when each NMES configuration was delivered
303 across a range of frequencies is shown in Figure 4A. There was a significant interaction between
304 NMES configuration and NMES frequency ($F_{(15, 210)} = 49.9, p < 0.001$). To test for differences
305 between NMES configurations at each frequency, separate one-way ANOVAs were run within
306 each frequency and significant main effects of NMES configuration were identified at 20 Hz ($F_{(3,$
307 $42)} = 52.1, p < 0.001$), 60 Hz ($F_{(3, 42)} = 24.1, p < 0.001$), 80 Hz ($F_{(3, 42)} = 37.6, p < 0.001$), 100 Hz ($F_{(3,$
308 $42)} = 35.3, p < 0.001$) and 120 Hz ($F_{(3, 42)} = 28.2, p < 0.001$). All significant differences in pairwise
309 comparisons for each frequency of NMES are shown in the lower portion of 4A. To summarise,
310 NMES₄ and NMES₈ evoked more torque than NMES₁ and NMES₂ at all frequencies above 40
311 Hz ($p < 0.05$), torque was only different between NMES₄ and NMES₈ at 100 Hz and 120 Hz
312 ($p < 0.05$) and torque was only different between NMES₁ and NMES₂ at 120 Hz ($p < 0.05$).

313 To test for differences between frequencies within each NMES configuration, separate

314 one-way ANOVAs were run within each NMES configuration and these identified significant
315 main effects of frequency for all configurations; NMES₁ ($F_{(5, 70)} = 75.9, p < 0.001$), NMES₂ ($F_{(5, 70)}$
316 $= 141.3, p < 0.001$), NMES₄ ($F_{(5, 70)} = 249.3, p < 0.001$) and NMES₈ ($F_{(5, 70)} = 81.7, p < 0.001$), as
317 shown in Figure 5A. For NMES₁ and NMES₂, torque reached a steady-state at 80 Hz, as torque
318 produced at 80, 100 and 120 Hz was not significantly different ($p > 0.05$). For NMES₄ and
319 NMES₈, torque reached a steady-state at 100 Hz ($p > 0.05$). The inset in Figure 4A shows the
320 range over which torque increased as NMES frequency increased from 20-120 Hz for each
321 configuration. There was a significant main effect of NMES configuration ($F_{(3, 42)} = 67.347,$
322 $p < 0.001$) and post-hoc tests showed that when NMES frequency increased from 20-120 Hz,
323 torque increased the least during NMES₁ (7% MVC), followed by NMES₂ (13% MVC), and
324 torque increased the most during NMES₄ and NMES₈ (21 and 24% MVC, respectively), which
325 were not different from each other ($p = 0.072$).

326

327 *Perceived discomfort*

328 *Current, current density and discomfort during the fatigue protocols*

329 There were significant differences in current used during the fatigue protocols between
330 NMES types ($F_{(3, 42)} = 6.893, p = 0.003$) as shown in Figure 5A. Significantly more current was
331 needed to generate the target 20% MVC contraction when using NMES₁ than NMES₄ ($p = 0.01$)
332 and NMES₈ ($p = 0.049$). There were also significant differences in current density between NMES
333 configurations ($F_{(3, 42)} = 54.6, p < 0.001$). Current density was higher during NMES₈ than all other
334 NMES configurations ($p \leq 0.001$) and was higher during NMES₁ than NMES₄ ($p = 0.001$) as
335 shown in Figure 5B.

336 There was no significant interaction between Time and NMES configuration for

337 discomfort during the fatigue protocols ($F_{(6, 84)} = 2.184, p=0.103$) and no main effect of Time
338 ($F_{(2,28)} = 2.128, p=0.138$) although there was a significant main effect of NMES configuration
339 ($F_{(3, 42)} = 9.916, p=0.001$). Pooled across the fatigue protocol, NMES₈ (40.4 ± 20.9) resulted in
340 significantly greater ratings of perceived discomfort than the other configurations ($p < 0.001$) as
341 shown in Figure 5C.

342

343 *Discomfort across frequencies*

344 Mean perceived discomfort scores recorded when the different NMES configurations
345 were delivered from 20-120 Hz are shown in Figure 4B. There was a significant interaction
346 between NMES type and frequency ($F_{(15, 195)} = 49.9, p=0.002$) and subsequent one-way
347 ANOVAs conducted to test for differences between configurations at each frequency identified
348 significant main effects of NMES configuration at 80 ($F_{(3, 39)} = 3.759, p=0.018$), 100 ($F_{(3, 39)} =$
349 $4.291, p < 0.010$) and 120 Hz ($F_{(3, 39)} = 5.704, p=0.002$). As shown in the bottom portion of Figure
350 4B, there were no differences in discomfort between NMES₁, NMES₂ and NMES₄ at any
351 frequency ($p > 0.05$). However, there was significantly more discomfort during NMES₈ at 80 Hz
352 and 100 Hz compared to the other configurations ($p < 0.05$) and at 120 Hz, NMES₈ produced more
353 discomfort than NMES₁, NMES₂ ($p < 0.05$).

354 Four 1 x 6 (Frequency) ANOVAs were run to test for an effect of frequency within each
355 NMES configuration and they indicated significant main effects of frequency for all
356 configurations; NMES₁ ($F_{(5, 65)} = 4.661, p=0.001$), NMES₂ ($F_{(5, 65)} = 4.402, p=0.002$), NMES₄
357 ($F_{(5, 65)} = 12.587, p < 0.001$) and NMES₈ ($F_{(5, 65)} = 10.878, p < 0.001$). Post hoc analyses showed
358 that discomfort was not significantly different between any two frequencies for NMES₁ and
359 NMES₂ ($p > 0.05$). For NMES₄, discomfort scores increased from 20 to 40 Hz and then reached a

360 steady state as there were no differences in discomfort between 40-120 Hz ($p>0.05$). During
361 NMES₈, discomfort increased up to 80 Hz and then reached a steady state. ($p>0.05$).

362

363 **DISCUSSION**

364 This study was designed to investigate the effect of rotating NMES pulses between an
365 increasing the number of stimulation channels (cathodes) on contraction fatigability, the
366 relationship between torque and NMES frequency and discomfort. Although contraction
367 fatigability did not decrease progressively as the number of cathodes increased, there was
368 significantly less fatigability when using more cathodes (NMES₄ and NMES₈) than fewer
369 cathodes (NMES₁ and NMES₂). Similarly, the amount of torque generated across a range of
370 NMES frequencies did not increase progressively as the number of cathodes increased, however,
371 the number of cathodes clearly influenced the relationship between torque and NMES frequency
372 and in general more cathodes produced more torque, particularly at the higher NMES
373 frequencies. Finally, NMES₈ caused the most discomfort, likely due to higher current density.
374 These results help establish the relationship between number of NMES channels and these
375 important outcome measures and suggest that delivering SDSS through 4 cathodes may be
376 optimal for reducing contraction fatigability of the quadriceps and producing large contractions
377 with minimal discomfort.

378

379 *Fatigability*

380 Contrary to our hypothesis, contraction fatigability did not decrease progressively as the
381 number of channels increased. Instead, contraction fatigability decreased when stimulus pulses
382 were rotated between 4 or 8 cathodes (NMES₄ and NMES₈), compared to delivering pulses

383 through a single fixed cathode (NMES₁) or alternating anode and cathode back and forth between
384 two electrodes (NMES₂). These differences in fatigability were evidenced by less decline in
385 torque and, on average, more torque over the 100 contractions of the fatigue protocols when
386 using NMES₄ and NMES₈ versus NMES₁ and NMES₂. SDSS has been shown previously to
387 reduce contraction fatigability for contractions of tibialis anterior (Wiest et al. 2019), triceps
388 surae (Nguyen et al. 2011) and quadriceps (Bergquist et al. 2017; Laubacher et al. 2017; Popović
389 and Malešević 2009; Malešević et al. 2010; Nguyen et al. 2011; Laubacher et al. 2019). The
390 reduced fatigability is thought to be due to reduced MU firing rates, afforded by the recruitment
391 of different pools of MUs from each spatially-distributed cathode (Nguyen et al. 2011; Sayenko
392 et al. 2014). However, in the present study there was no improvement in fatigability when
393 doubling the number of cathodes from 1 to 2 (NMES₁ to NMES₂) or from 4 to 8 (NMES₄ to
394 NMES₈). This lack of improvement in fatigability contrasts with improvements gained when
395 doubling the number of channels from 1 to 2 when stimulating tibialis anterior to dorsiflex the
396 ankle(Lou et al. 2017), and may be accounted for by the electrode configurations used in the
397 present study. The locations of the two electrodes used to deliver NMES₁ and NMES₂ were
398 identical, the only difference being that anode and cathode were “fixed” during NMES₁, and
399 were alternated between the two electrodes during NMES₂. Thus, the path for current flow was
400 the same during both protocols, and despite alternating the cathode between electrodes, NMES₂
401 may have recruited the same MUs with each pulse, effectively rendering NMES₁ and NMES₂
402 equivalent in terms of MU discharge rates and contraction fatigability. Accordingly, approaches
403 that alternate anode and cathode between the same two electrodes may not be effective to reduce
404 contraction fatigability. Similarly, configurations for NMES₄ and NMES₈ occupied the same area
405 on the thigh and, other than number of cathodes, the difference for NMES₈ was that the

406 electrodes were half the size as for the other configurations. Thus, during NMES₈ there was
407 likely a high overlap of MUs recruited by adjacent cathodes, effectively making adjacent pairs a
408 single electrode and thus NMES₄ and NMES₈ equivalent in terms of MU discharge rates and
409 fatigability. Together the present results suggest that for reducing contraction fatigability of the
410 quadriceps, alternating anode and cathode between the same electrodes is not sufficient to reduce
411 contraction fatigability, instead, an SDSS approach may be best and presently we show that
412 rotating pulses through 4 or 8 cathodes is equally effective and better than 1 or 2.

413

414 *Torque-frequency relationships*

415 Contrary to our hypothesis, increasing the number of cathodes did not progressively
416 increase the amount of torque produced over a range of NMES frequencies, although the number
417 of cathodes clearly influenced the relationship between torque and frequency. When NMES
418 frequency increased from 10–120 Hz, torque increase 7, 13, 21 and 24% MVC using NMES₁,
419 NMES₂, and NMES₄ and NMES₈ (which were not different), respectively. NMES₄ and NMES₈
420 evoked more torque than NMES₁ and NMES₂ at all frequencies above 40 Hz and further
421 differences between configurations emerged at the highest NMES frequencies. NMES₈ produced
422 more torque than NMES₄ at 100 and 120 Hz and NMES₂ generated more torque than NMES₁ at
423 120 Hz. Thus, at the highest frequency tested (120 Hz), torque increased progressively with the
424 number of cathodes, consistent with our hypothesis. The differences that emerged between
425 configurations at the highest frequencies suggest there are subtle differences how MUs are
426 recruited between these configurations but they are not sufficient to measurably influence
427 contraction fatigability.

428 We propose that the differences in torque-frequency relationships between configurations

429 are due to recruiting more MUs, at progressively lower rates, as number of channels increase.
430 The lower firing rates place MUs progressively leftward on their torque-frequency curves. Thus,
431 as the number of channels increase, there is a wider range over which increases in NMES
432 frequency produce increases in torque. The ability of SDSS to reduce MU firing rates, while still
433 being delivered at sufficiently “net” frequencies to produce large contractions, provides a unique
434 opportunity to remove two of the main impediments to the widespread use of NMES, contraction
435 fatigability and the inability to produce sufficiently large contractions.

436

437 *Current and discomfort*

438 Although significantly less current was required to evoke the target contractions of 20%
439 MVC when rotating pulses between 4 or 8 cathodes (NMES₄ and NMES₈), than when
440 stimulating through a single fixed cathode (NMES₁), the smaller electrode size necessitated
441 when using 8 cathodes resulted in significantly higher current density than the other three
442 configurations. This higher current density corresponded to the highest ratings of perceived
443 discomfort for NMES₈ during the fatigue protocols and at the higher NMES frequencies used to
444 generate the torque-frequency curves. These results are consistent with previous work indicating
445 that higher current densities increase discomfort during NMES (Alon 1985; Patterson and
446 Lockwood 1991; Maffiuletti 2010). Smaller electrodes were required during NMES₈ due to
447 limitations in space over the quadriceps which poses a limitation moving forward with higher
448 channel numbers and for smaller muscles as discomfort limits the use of NMES (Barss et al.
449 2018). Of note, however, is that SDSS through 4 cathodes has proven to reduce contraction
450 fatigability for contractions of tibialis anterior, a muscle with markedly less surface area for
451 stimulation (Wiest et al. 2019). Considering that fatigability was similar between NMES₄ and

452 NMES₈ but discomfort during NMES₄ was less than NMES₈ and was not different than NMES₁
453 and NMES₂, NMES₄ may provide most clinically meaningful balance between reducing both
454 fatigability and discomfort.

455

456 *Applications, limitations, and future directions*

457 Rotating stimulus pulses between multiple channels over a muscle during NMES
458 provides a readily translatable advancement to improve outcomes of NMES-based programs and
459 reduce secondary complications that stem from inactivity. Despite the potential for further
460 refinements (see below), four-channel SDSS, as described in this and other studies (Nguyen et al.
461 2011; Sayenko et al. 2014; Bergquist et al. 2017; Wiest et al. 2019), produces larger and more
462 fatigue-resistant contractions than conventional NMES and could be relatively-easily
463 incorporated into NMES-based programs. Indeed, 4-channel SDSS over the quadriceps enables
464 individuals with a complete spinal cord injury to cycle 3x longer than when using conventional
465 NMES (Barss TS, *unpublished observation*). Future research involving longitudinal training
466 studies is needed to determine the extent to which SDSS improves relevant musculoskeletal and
467 cardiovascular outcomes of NMES-based programs compared to conventional NMES
468 approaches.

469 Although the electrode configurations used in the present study were based on pilot
470 experiments designed to identify configurations that reduced contraction fatigability by
471 minimizing MU overlap between adjacent electrodes, the configurations chosen may not be
472 optimal. Accordingly, further exploration to identify optimal electrode number and configuration
473 will be important to maximise the potential of SDSS. The optimal configuration will be the one
474 that maximises MU recruitment (i.e. recruits the highest percentage of MUs in the target muscle)

475 and minimises overlap of MUs recruited by adjacent electrodes. Randomising the order of
476 stimulation between channels, changing the placement of the anode, rotating anode-cathode
477 pairs, and orienting channels to target separate MUs to decrease overlap all remain as potential
478 strategies to reduce contraction fatigability, reduce discomfort and increase evoked torque.

479 SDSS offers a unique opportunity to maintain low MU discharge rates, by delivering
480 stimulus pulses to each channel at relatively low frequencies (“net” frequency / number of
481 channels), while still generating large contractions, as the forces generated by separate pools of
482 MUs recruited by each channel sum at the tendon at the net frequency of stimulation. For
483 example, discomfort issues aside, delivering NMES₈ at 120 Hz would take advantage of the
484 opportunity to generate large contractions, due to the high “net” frequency, while still
485 maintaining MU firing rates within their physiological range with pulses delivered at 15 Hz to
486 each channel. Indeed, had each type of NMES been delivered at a net frequency of 120 Hz for
487 the fatigue protocols in the present study there may have been a markedly greater effect of
488 channel number on fatigability. Future research is needed to identify the optimal frequency for
489 SDSS that provides a compromise between the high frequencies needed to generate large
490 contractions and the low frequencies that minimise fatigability. It may be that different
491 frequencies are optimal for different applications or even at different times within a given
492 setting. The high net frequencies that are feasible during SDSS, while still minimizing
493 contraction fatigability, may also have the added benefit of sending a relatively large
494 neuromodulatory signal to the central nervous system, by the stimulation of sensory axons,
495 which may promote beneficial neuroplasticity within central nervous system.

496

497

498 *Conclusions*

499 Rotating NMES pulses between an increasing number of cathodes over the quadriceps
500 muscles did not progressively reduce contraction fatigability or increase the ability to generate
501 torque across a range of frequencies. Rotating pulses between 4 or 8 cathodes did, however,
502 reduce contraction fatigability and generate more torque across frequencies than when using 1 or
503 2 cathodes. Delivering NMES through 8 cathodes required smaller electrodes than for the other
504 configurations which increased current density and perceived discomfort. Thus, during NMES,
505 more stimulation channels are not necessarily better, and rotating pulses between 4 cathodes may
506 be optimal to minimize contraction fatigability and generate large contractions with minimal
507 discomfort.

508

509

510

511

512

513

514

515

516

517

518

519

520

521 *References*

522 Alon G (1985) High voltage stimulation. Effects of electrode size on basic excitatory responses.

523 *Phys Ther* 65:890–5

524 Barss TS, Ainsley EN, Claveria-Gonzalez FC, et al (2018) Utilising physiological principles of

525 motor unit recruitment to reduce fatigability of electrically-evoked contractions : A

526 narrative review. *Arch Phys Med Rehabil* 99:779–791.

527 <https://doi.org/10.1016/j.apmr.2017.08.478>

528 Bélanger M, Stein RB, Wheeler GD, et al (2000) Electrical stimulation: Can it increase muscle

529 strength and reverse osteopenia in spinal cord injured individuals? *Arch Phys Med Rehabil*

530 81:1090–1098. <https://doi.org/10.1053/apmr.2000.7170>

531 Bergquist AJ, Babbar V, Ali S, et al (2017) Fatigue reduction during aggregated and distributed

532 sequential stimulation. *Muscle and Nerve* 56:271–281. <https://doi.org/10.1002/mus.25465>

533 Bergquist AJ, Clair JM, Lagerquist O, et al (2011) Neuromuscular electrical stimulation:

534 Implications of the electrically evoked sensory volley. *Eur J Appl Physiol* 111:2409–2426.

535 <https://doi.org/10.1007/s00421-011-2087-9>

536 Bickel CS, Gregory CM, Dean JC (2011) Motor unit recruitment during neuromuscular electrical

537 stimulation: A critical appraisal. *Eur J Appl Physiol* 111:2399–2407.

538 <https://doi.org/10.1007/s00421-011-2128-4>

539 Davis GM, Hamzaid NA, Fornusek C (2008) Cardiorespiratory, metabolic, and biomechanical

540 responses during functional electrical stimulation leg exercise: Health and fitness benefits.

541 *Artif Organs* 32:625–629. <https://doi.org/10.1111/j.1525-1594.2008.00622.x>

542 Fukuda TY, Marcondes FB, Dos Anjos Rabelo N, et al (2013) Comparison of peak torque,

543 intensity and discomfort generated by neuromuscular electrical stimulation of low and

544 medium frequency. *Isokinet Exerc Sci* 21:167–173. <https://doi.org/10.3233/IES-130495>

545 Griffin L, Decker MJ, Hwang JY, et al (2009) Functional electrical stimulation cycling improves
546 body composition, metabolic and neural factors in persons with spinal cord injury. *J*
547 *Electromyogr Kinesiol* 19:614–622. <https://doi.org/10.1016/j.jelekin.2008.03.002>

548 Kluger BM, Lauren Krupp MB, Enoka RM, et al (2013) Fatigue and fatigability in neurologic
549 illnesses: Proposal for a unified taxonomy. *Neurology* 80:409–416.
550 <https://doi.org/10.1212/WNL.0b013e31827f07be>

551 Laubacher M, Aksoez EA, Brust AK, et al (2019) Stimulation of paralysed quadriceps muscles
552 with sequentially and spatially distributed electrodes during dynamic knee extension. *J*
553 *Neuroeng Rehabil* 16:1–12. <https://doi.org/10.1186/s12984-018-0471-y>

554 Laubacher M, Aksöz AE, Riener R, et al (2017) Power output and fatigue properties using
555 spatially distributed sequential stimulation in a dynamic knee extension task. *Eur J Appl*
556 *Physiol* 117:1787–1798. <https://doi.org/10.1007/s00421-017-3675-0>

557 Lou JWH, Bergquist AJ, Aldayel A, et al (2017) Interleaved neuromuscular electrical
558 stimulation reduces muscle fatigue. *Muscle and Nerve* 55:179–189.
559 <https://doi.org/10.1002/mus.25224>

560 Maffiuletti NA (2010) Physiological and methodological considerations for the use of
561 neuromuscular electrical stimulation. *Eur J Appl Physiol* 110:223–234.
562 <https://doi.org/10.1007/s00421-010-1502-y>

563 Malešević NM, Popović LZ, Schwirtlich L, Popović DB (2010) Distributed low-frequency
564 functional electrical stimulation delays muscle fatigue compared to conventional
565 stimulation. *Muscle and Nerve* 42:556–562. <https://doi.org/10.1002/mus.21736>

566 Nguyen R, Micera S, Morari M, et al (2011) Spatially Distributed Sequential Stimulation

567 Reduces Fatigue in Paralyzed Triceps Surae Muscles: A Case Study. *Artif Organs* 35:1174–
568 1180. <https://doi.org/10.1111/j.1525-1594.2010.01195.x>

569 Patterson RP, Lockwood JS (1991) The Current Requirements And The Pain Response For
570 Various Sizes Of Surface Stimulation Electrodes. *Eng Med Biol Soc* 1991 Vol 13 1991,
571 *Proc Annu Int Conf IEEE* 13:1809–1810

572 Popović LZ, Malešević NM (2009) Muscle fatigue of quadriceps in paraplegics: Comparison
573 between single vs. multi-pad electrode surface stimulation. *Proc 31st Annu Int Conf IEEE*
574 *Eng Med Biol Soc Eng Futur Biomed EMBC 2009* 6785–6788.
575 <https://doi.org/10.1109/IEMBS.2009.5333983>

576 Sayenko DG, Nguyen R, Hirabayashi T, et al (2014) Method to reduce muscle fatigue during
577 transcutaneous neuromuscular electrical stimulation in major knee and ankle muscle groups.
578 *Neurorehabil Neural Repair* 1– 12. <https://doi.org/10.1177/1545968314565463>

579 Sheffler LR, Chae J (2007) Neuromuscular electrical stimulation in neurorehabilitation. *Muscle*
580 *Nerve* 35:562–90. <https://doi.org/10.1002/mus.20758>

581 Wiest MJ, Bergquist AJ, Heffernan MG, et al (2019) Fatigue and Discomfort During Spatially
582 Distributed Sequential Stimulation of Tibialis Anterior. *IEEE Trans Neural Syst Rehabil*
583 *Eng* 27:1566–1573. <https://doi.org/10.1109/TNSRE.2019.2923117>

584

585

586

587

588

589

590 *Figure legends*

591 **Figure 1. Electrode placements and experimental protocol.** Panel (A) shows the placement of
592 electrodes over the quadriceps where letters represent anodes and numbers represent cathodes.
593 Stimulus pulses were delivered to cathodes sequentially in the numerical order represented on
594 the diagram. During NMES₂, the cathode (and anode) alternated between positions 1 and 2 with
595 each pulse. During NMES₄, proximal cathodes (1, 3) were paired with anode A and distal
596 cathodes (2, 4) were paired with anode B. Similarly, during NMES₈, proximal cathodes (1, 3, 5,
597 7) were paired with anode A and distal cathodes (2, 4, 6, 8) were paired with anode B. Panel (B)
598 shows the timeline of the protocol used for each experiment divided into PRE, FATIGUE and
599 POST phases. Torque recorded during the first 10 (Bin 1) and last 10 (Bin 10) contractions of a
600 fatigue protocol are shown for a representative participant in Panel (C).

601

602 **Figure 2. Data recorded one participant during the fatigue protocols.** Panel (A) shows
603 torque recorded during all 100 contractions of each fatigue protocol. These data are also shown
604 in Panel (B) where the mean torque during each contraction was averaged over 10 successive
605 contractions to form 10 bins for each NMES configuration.

606

607 **Figure 3. Group data recorded during the fatigue protocols and associated measures of**
608 **contraction fatigability.** Panel (A) shows torque recorded during the fatigue protocols using
609 each configuration, binned and averaged across participants. Percent change in mean torque and
610 the torque-time integral (TTI) from the first 10 contractions (bin 1) to the last 10 contractions
611 (bin 10) of the fatigue protocols, are shown in panel (B) and panel (C), respectively. Average
612 torque (D) and TTI (E) calculated over the 10 bins. Significant differences are indicated by the

613 pound symbols (#). Open circles represent data from individual participants. Data are presented
614 as mean \pm SD.

615

616 **Figure 4. Group data showing torque-frequency and discomfort-frequency relationships**

617 **for each NMES configuration.** Panel (A) shows torque produced when each NMES

618 configuration was delivered at frequencies from 20 Hz to 120 Hz. The dagger symbol (†)

619 indicates the frequency at which torque produced by NNMES₄ and NMES₈ was not different

620 than torque that each produced at 120 Hz. Double daggers (‡) indicate the frequency at which

621 torque produced by NMES₁ and NMES₂ was not different than that each produced at 120 Hz.

622 Comparisons between configurations at each a frequency are shown below the x axis below their

623 corresponding frequency. In these graphs the pound symbol (#) denotes significant differences as

624 indicated and asterisks (*) denote a significant difference from all other configurations. The inset

625 in the top left corner shows the increase in torque produced by each configuration when NMES

626 frequency increased from 20-120 Hz. Panel (B) shows perceived discomfort assessed at each

627 frequency using a Visual Analogue Scale (VAS). Double daggers († †) indicate the frequency at

628 which VAS scores for NMES₈ were not different than scores at 120 Hz and the four daggers (‡‡)

629 indicate the frequency at which VAS scores for NMES₄ were not different than scores that at 120

630 Hz. Comparisons between configurations at each a frequency are shown below the x axis in the

631 same format as for Panel A. In both panels data are presented as mean \pm SD.

632

633 **Figure 5. Group data showing current, current density and perceived discomfort during**

634 **the fatigue protocols.** Panel (A) shows the mean current and Panel (B) shows the current density

635 used to generate the contractions for the fatigue protocols using each NMES configuration. VAS

636 scores in Panel (C) represent the pooled mean of scores from the 5th, 50th and 95th contractions of
637 the fatigue protocols for each participant. Pound symbols (#) denote significant differences as
638 indicated and asterisks (*) denote significant differences from all other configurations. Open
639 circles represent data from individual participants. Data are presented as mean \pm SD.

Figures

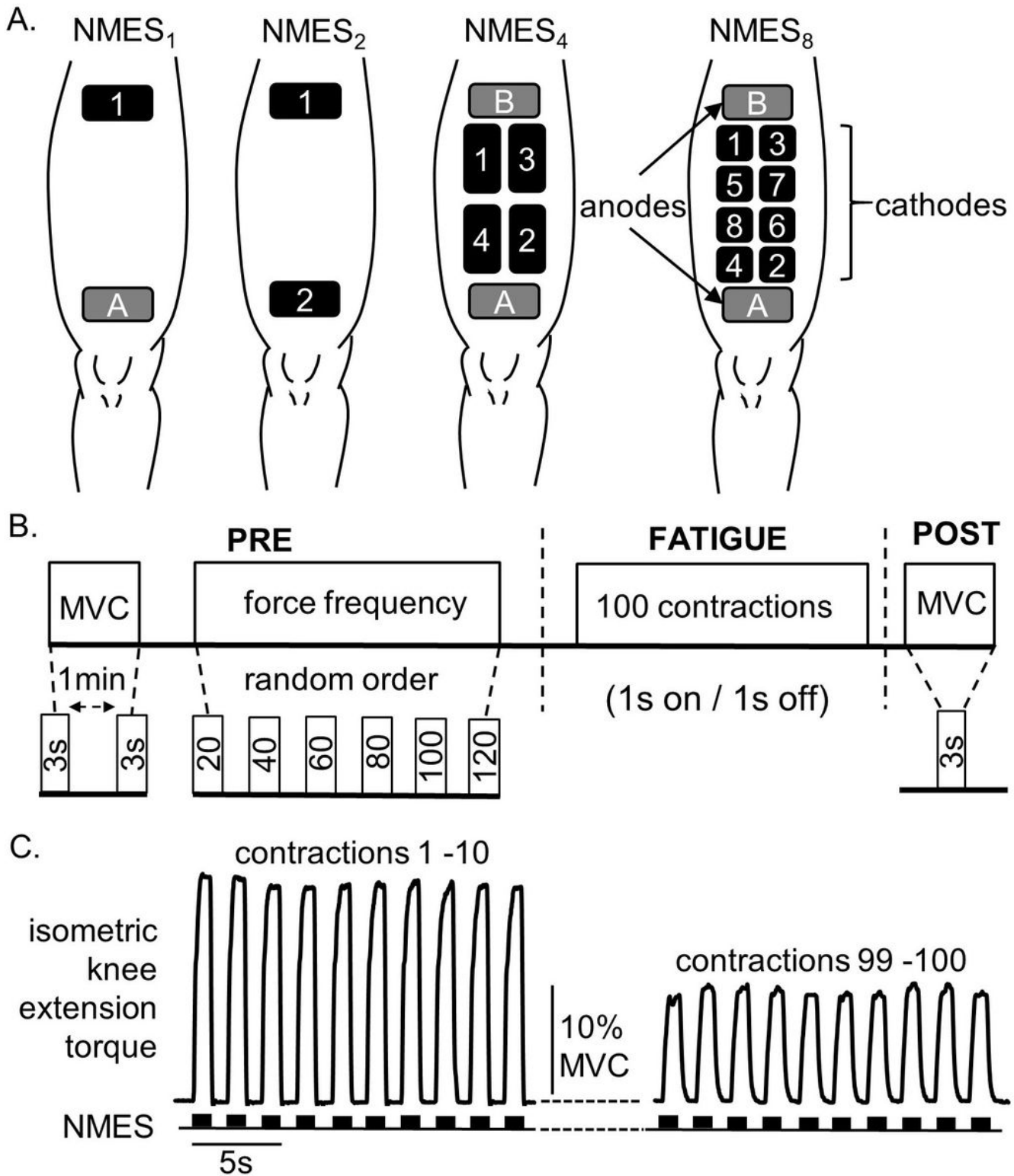


Figure 1

Electrode placements and experimental protocol. Panel (A) shows the placement of electrodes over the quadriceps where letters represent anodes and numbers represent cathodes. Stimulus pulses were delivered to cathodes sequentially in the numerical order represented on the diagram. During NMES2, the

cathode (and anode) alternated between positions 1 and 2 with each pulse. During NMES₄, proximal cathodes (1, 3) were paired with anode A and distal cathodes (2, 4) were paired with anode B. Similarly, during NMES₈, proximal cathodes (1, 3, 5, 7) were paired with anode A and distal cathodes (2, 4, 6, 8) were paired with anode B. Panel (B) shows the timeline of the protocol used for each experiment divided into PRE, FATIGUE and POST phases. Torque recorded during the first 10 (Bin 1) and last 10 (Bin 10) contractions of a fatigue protocol are shown for a representative participant in Panel (C).

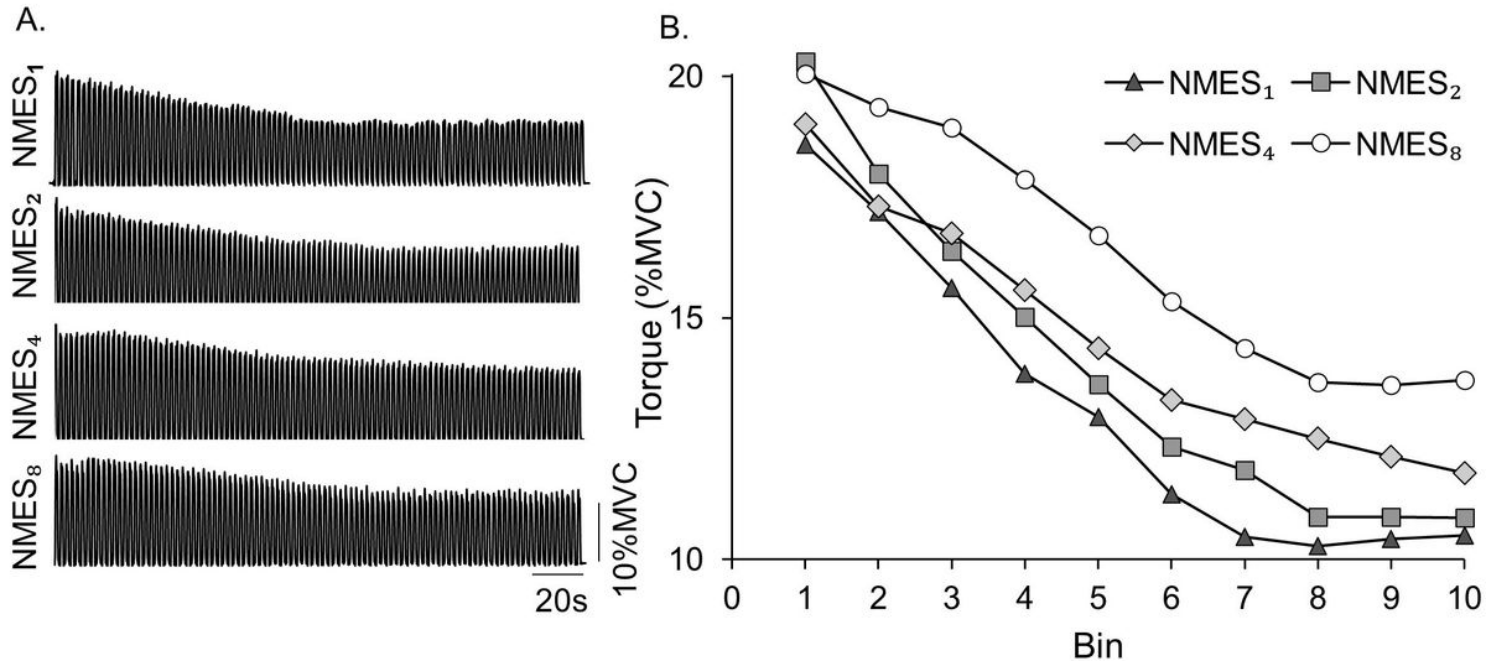


Figure 2

Data recorded one participant during the fatigue protocols. Panel (A) shows torque recorded during all 100 contractions of each fatigue protocol. These data are also shown in Panel (B) where the mean torque during each contraction was averaged over 10 successive contractions to form 10 bins for each NMES configuration.

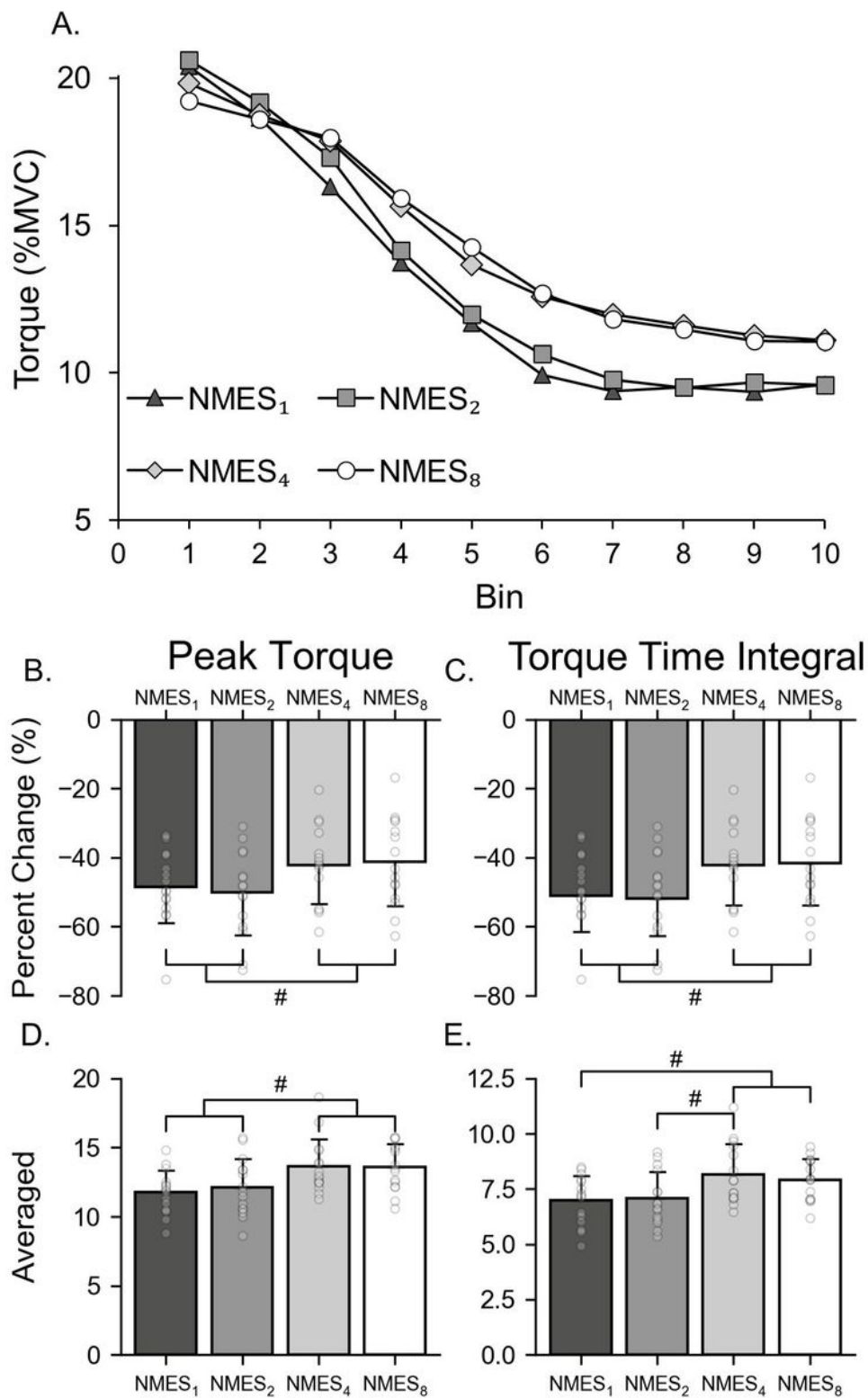


Figure 3

Group data recorded during the fatigue protocols and associated measures of contraction fatigability. Panel (A) shows torque recorded during the fatigue protocols using each configuration, binned and averaged across participants. Percent change in mean torque and the torque-time integral (TTI) from the first 10 contractions (bin 1) to the last 10 contractions (bin 10) of the fatigue protocols, are shown in panel (B) and panel (C), respectively. Average torque (D) and TTI (E) calculated over the 10 bins.

Significant differences are indicated by the pound symbols (#). Open circles represent data from individual participants. Data are presented as mean \pm SD.

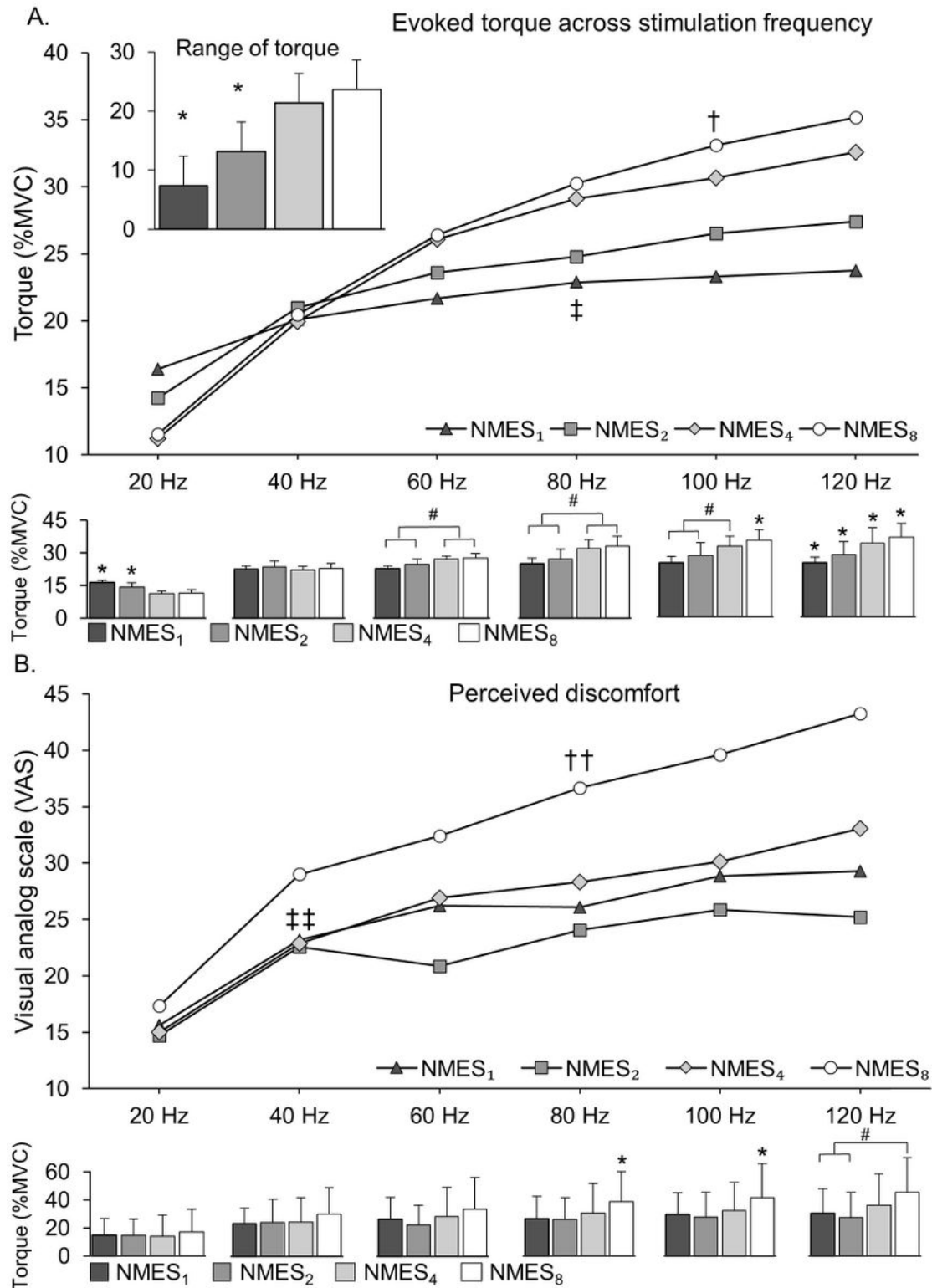


Figure 4

Group data showing torque-frequency and discomfort-frequency relationships for each NMES configuration. Panel (A) shows torque produced when each NMES configuration was delivered at frequencies from 20 Hz to 120 Hz. The dagger symbol (†) indicates the frequency at which torque

produced by NNMES4 and NMES8 was not different than torque that each produced at 120 Hz. Double daggers (‡) indicate the frequency at which torque produced by NMES1 and NMES2 was not different than that each produced at 120 Hz. Comparisons between configurations at each a frequency are shown below the x axis below their corresponding frequency. In these graphs the pound symbol (#) denotes significant differences as indicated and asterisks (*) denote a significant difference from all other configurations. The inset in the top left corner shows the increase in torque produced by each configuration when NMES frequency increased from 20-120 Hz. Panel (B) shows perceived discomfort assessed at each frequency using a Visual Analogue Scale (VAS). Double daggers († †) indicate the frequency at which VAS scores for NMES8 were not different than scores at 120 Hz and the four daggers (‡‡) indicate the frequency at which VAS scores for NMES4 were not different than scores that at 120 Hz. Comparisons between configurations at each a frequency are shown below the x axis in the same format as for Panel A. In both panels data are presented as mean \pm SD.

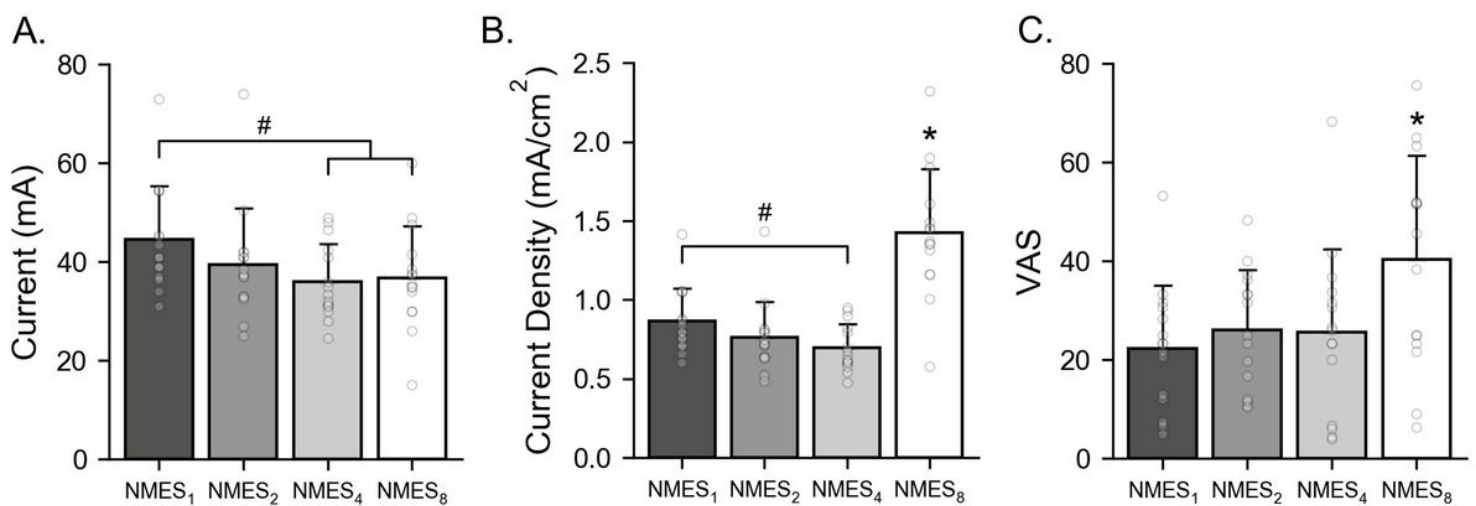


Figure 5

Group data showing current, current density and perceived discomfort during the fatigue protocols. Panel (A) shows the mean current and Panel (B) shows the current density used to generate the contractions for the fatigue protocols using each NMES configuration. VAS scores in Panel (C) represent the pooled mean of scores from the 5th, 50th and 95th contractions of the fatigue protocols for each participant. Pound symbols (#) denote significant differences as indicated and asterisks (*) denote significant differences from all other configurations. Open circles represent data from individual participants. Data are presented as mean \pm SD.